Asian Journal of Chemistry; Vol. 30, No. 7 (2018), 1559-1563

ASIAN JOURNAL OF CHEMISTRY

https://doi.org/10.14233/ajchem.2018.21242

Optimization Properties and Characterization of Green Synthesis of Copper Oxide Nanoparticles Using Aqueous Extract of *Cordia myxa* L. Leaves

N.A. THAMER[1,*], N.Q. MUFTIN[2] and S.H.N. AL-RUBAE[2]

[1]Department of Molecular Biology, Iraqi Center for Cancer and Medical Genetic Research, Al-Mustansiriyah University, Al-Qadisia, Baghdad, Iraq
[2]College of Science, Al-Mustansiriyha University, Palastin Street, Al Mustansiriyah Square, Baghdad, Iraq

*Corresponding author: Tel: +964 7804234134; E-mail: neran1958@yahoo.com

Received: 19 January 2018; *Accepted*: 7 March 2018; *Published online*: 31 May 2018; AJC-18930

Copper oxide nanoparticles (CuONPs) were green synthesized using aqueous extract of *Cordia myxa* L. leaves as reducing and capping agent. The synthesized nanoparticles were characterized by UV-visible spectrophotometer, FTIR, X-ray diffraction, scanning electron microscope and atomic force microscope. The prepared copper oxide nanoparticles showed surface plasmon resonance centered at 400 nm. The optimized condition for the synthesis of copper nanoparticles revealed that the aqueous extract of *Cordia myxa* L. leaves:copper sulfate ratio was 1:3, pH was 9 and copper sulfate concentration was 40 mM. FTIR results showed that stabilization and formation of CuONPs were due to phenolic groups and amines in plant extract. The XRD pattern showed that the particles are monoclinic in nature. The crystalline morphology and size of the nanoparticles were determined by scanning electron microscope. Presence of elemental copper was revealed by EDX analysis. Size range was from 20 to 106.81 nm was determined by atomic force microscope.

Keywords: *Cordia myxa* L., Copper oxide nanoparticles, XRD, Scanning electron microscope, Atomic force microscope.

INTRODUCTION

Nanotechnology is an important branch in the major field of science. It concerned with the synthesis and development of various types of nanoparticles with size range from 1 to 100 nm [1]. It is noted that physical and chemical properties of any materials changes with it size decreased to nanoscale [2]. Nanosized particles show variations of optical, electrical and magnetic properties compared with bulk size of the same material [3].

Their characters depended on certain trait such as size particle, distribution, morphology [4] and high surface/volume ratio [5]. Metal oxide nanoparticles obtained great attention for their potential applications in optoelectronics, nanodevices, nanoelectronics, nanosensors, information storage and catalysis [6,7]. Among various metal oxide nanoparticles, the copper oxide was implemented in wide range of application. It can be used as catalysts in reduction, oxidation electrocatalysis, photocatalysis and gas-phase reaction [8].

Biological methods to synthesize nanoparticles using fungi, bacteria, algae [9] and plant extracts have many advantages over other physical and chemical methods because they are a single step process in nature, environment friendly (green chemistry), no need for, hazardous chemicals, high pressure or energy and power [10]. Moreover, plant leaf extracts appear to be the best candidates for synthesis of nanoparticles [11].

Plant extracts are becoming favourable sources as reducing and stabilizing agent for green synthesis of nanoparticles [12]. *Cordia myxa* L. is a species of flowering plant in the borage family, Boraginaceae. It generally had analgesic, anti-inflammatory, antimicrobial, antiparasitic and insecticidal. It also has a cardiovascular, respiratory, gastrointestinal protective effects [13]. In the present study the synthesis of copper oxide nanoparticles confirms the capability of *Cordia myxa* L. in reducing and stabilizing copper oxide nanoparticles. Their properties were investigated using different characterization techniques.

EXPERIMENTAL

Fresh leaves of *Cordia myxa* L. were collected in May, 2016 during the flowering season from the local gardens in Baghdad. The collected leaves material were tightly packed in polyethylene bag and then transferred to the laboratory. Then, the leaves were washed with distilled water twice and stored at room temperature. Dried leaves were powdered using mixer grinder. It was then stored in any dry place for further use.

Preparation of plant leaf extract: 5 g of powdered leaves were taken in a round flask along with 100 mL of deionized water, allowed to boil at 70 °C for 45 min under reflux condition and then cooled down to room temperature. The extract obtained was filtered through Whatman No. 1 filter paper. The filtrate was stored at 4 °C for further experiments.

Preparation of copper oxide nanoparticles: For synthesis of copper oxide nanoparticles, 40 mM $CuSO_4 \cdot 5H_2O$ (Sigma-Aldrich Company, USA) solution was added to the heated plant extract at the proper ratio and left at room temperature overnight. The change in colour from brown to green was indicating of the formation of copper oxide nanoparticles. The content was centrifuged at 4000 rpm for 15 min, washed with distilled water and dried at room temperature [14]. To study the optimum conditions for CuONPs synthesis, the experiments were carried out with different copper sulphate to *Cordia myxa* L. aqueous extract ratio (1:1, 1:2, 1:3, 1:4 and 1:5), pH (3, 5, 7, 9 and 11) and the copper ion concentration (10, 20, 30, 40 and 50 mM). The pH of the reaction was adjusted using 0. 1 N NaOH and 0.1 N HCl. The effect of these parameters on the synthesis CuONPs was monitored by UV-visible spectrophotometer.

Characterization of green synthesis copper oxide nanoparticles

UV spectral analysis: The synthesized CuONPs were initially characterized by UV-visible spectrophotometer to confirm its presence. Ultra violet spectral measurement was carried out in range of wavelength between 300-700 nm by double beam UV-visible spectrophotometer (PD-303 UV).

Fourier transform infrared spectral analysis: The FT-IR spectra was detected (Shimadzu IR-Prestige 21) to identify the bioactive molecules responsible for the reduction of copper ions with capping ability of the bioreduced CuONPs. The spectra was recorded in the wavelength interval 4000-400 cm^{-1}.

X-ray diffraction studies: X-ray diffraction measurements of CuO NPs was carried out using X-ray diffractometer instrument [Shimadzu XRD-6000, AS (3k.NOPC)], an angle range between 30-80° with CuK_α radiation in a θ-2θ configuration. The average crystallite size of the CuONPs calculated by Debye-Scherrer formula as, $D = k\lambda/\beta\cos\theta$, where D is particle diameter size, k is a constant equals 0.94, λ is wavelength of X-ray source (0.1541 Å), β is the full width at half maximum (FWHM) and θ is the Bragg angle [15].

Scanning electron microscopy energy & dispersive X-ray spectroscopy: The mean particle size of the synthesized CuONPs was determined by SEM analysis. SEM measurement was performed on INSPECT S50 FEI. The presence of elemental copper was confirmed through EDX. The EDX observations were carried out by EDX detector coupled with SEM.

Atomic force microscopy: Shape and size distribution of the formulated CuONPs was studied by atomic force microscopy (Phywenano compact AFM).

RESULTS AND DISCUSSION

Colour change: Change in colour mixture of leave extract and copper sulphate to dark green after overnight reaction clearly indicates the formation of CuONPs. This formation was characterized by the UV-visible spectroscopy analysis to confirm the presence of specific surface plasmon resonance (SPR) [16]. In the UV-visible spectrum peak at 392 nm was noticed due to SPR of metal oxide (Fig. 1). This wavelength was closely matched the others reported value [17]. Another researcher have reported that the synthesis of CuONPs can be monitored by the formation of SPR at 415 nm [18]. Various reports have established that the SPR band of copper nanoparticles were observed between 620 to 710 nm [19]. These variations in the SPR may be attributed to spherical shape of copper oxide nanoparticles, the surface plasmon resonance and the blue shift are affected by the size distribution [20]. According to Mie's theory only a single SPR band is expected in the absorption spectra of spherical metal nanoparticles [21]. In the present study a single SPR peak was observed assuming that the synthesized CuONPs were spherical in shape.

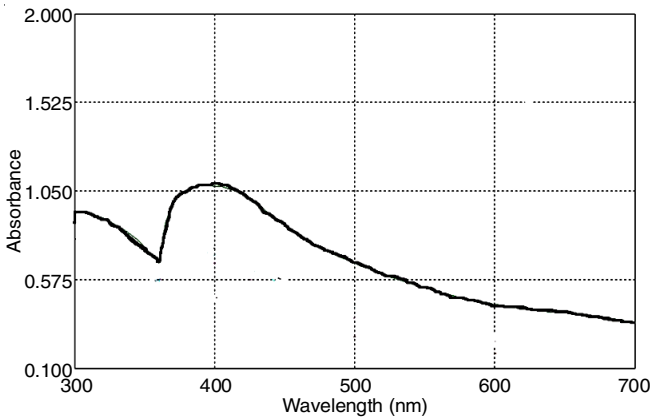

Fig. 1. UV-visible spectra of copper oxide nanoparticles, showed a strong SPR which was centered at 400 nm

Different parameters were optimized for the biosynthesis of copper nanoparticles

Volume ratio of extract and copper sulphate: The formation of copper oxide nanoparticle depends on the ratio of extract/$CuSO_4$ (v/v). The UV-visible spectrum was recorded for the shift in SPR peaks position with variation in the amount of extract to precursor salt as shown in the Fig. 2. A red shift in the wavelength from 365 to 369 nm was observed with the increase in the volume of extract from 1:1 to 1:2 and then further increase in red shift from 369 to 392 nm by an increase of the ratio to 1:3. The SPR variation may be attributed to influence between smaller nanoparticles which leads to particles growth [22]. The accurate position of the SPR band could differ depending on the size, shape and capping agent, among other individuals properties of the nanoparticles [23,24]. The maximum absorption was observed at 1:3 ratio, but by increasing the ratio to 1:4 and 1:5 v/v, the absorption decreased. The 1:3 ratio was found to be typical to biosynthesize nanoparticles, it showed maximum absorption at 394 nm which was in assent with the values reported in the literature [25].

Effect of pH: Green synthesis of copper oxide nanoparticles using aqueous extract of *Cordia myxa* L. leaves was examined over a broad pH range (3-11). Variations in pH were highly affected the SPR of CuONPs. Moreover, the influence of pH on the proceed of reduction reaction has also been

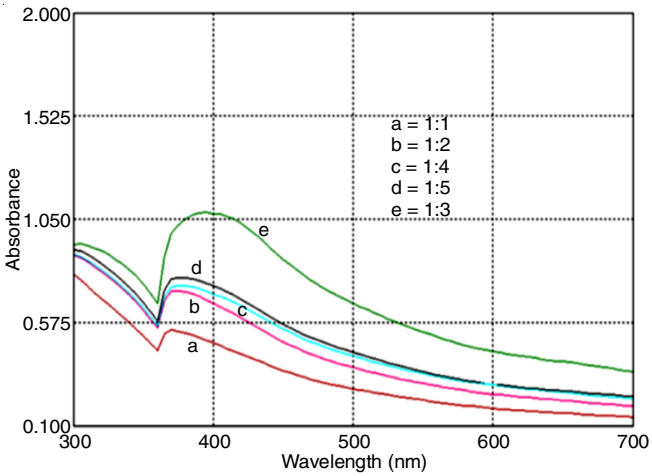

Fig. 2. Effect of different ratio for *Cordia myxa* aqueous extract/copper sulphate on CuONPs formation indicate the optimum ratio was 1:3

reported by many literatures [26,27]. As shown in Fig. 3, increasing in pH from 3 to 7, the SPR was increased from 372 to 376 nm. A red shift in the wavelength was observed from 376 to 400 nm with the increase in pH from 7 to 9. Absorption in UV-visible spectra was the maximum in pH 9. The increase in pH from 9 to 11 decreased the absorption. The pH was one of the factors that influenced the size, shape and composition of a nanoparticle [28]. In acidic pH, nanoparticles aggregated out of the nucleation, while at alkaline pH, great numbers of nuclei formed, instead of aggregation [29,30]. So pH 9 was found to be optimum to biosynthesize nanoparticles, which was in a match the values reported in the literature [19].

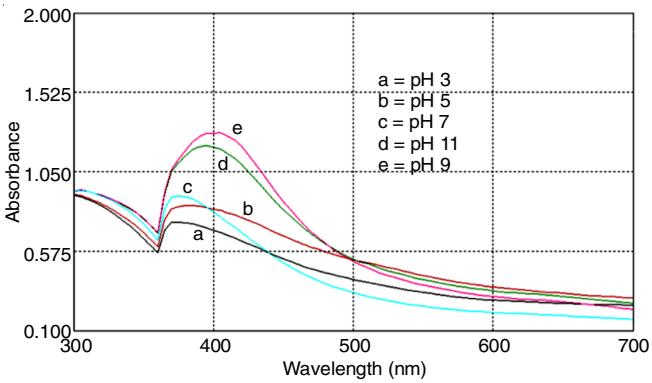

Fig. 3. Effect of different pH on CuONPs formation. The optimum pH was 9

Different concentration of copper sulphate: Formation of copper oxide nanoparticles was studied by the variation of copper sulphate concentration from 10 to 50 mM. The SPR absorption was increased due to increasing the concentration of copper ions from 10 to 40 mM (Fig. 4). This may be attributed to the formation of more CuONPs as the reaction progresses since the intensity of the surface plasmon peak is directly proportional to the density of the CuONPs in solution. It can be assumed that at both lower 10 mM and higher 40 mM concentration of copper sulphate not sufficient nuclei were shaped. As increasing in the concentration of copper sulphate more than 40 mM the SPR absorbance decrease that could be due to the low number of reducing agent molecules. In the case of

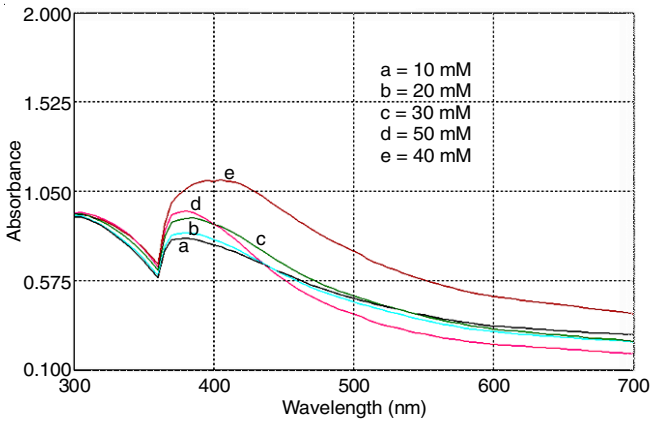

Fig. 4. UV spectrum of green synthesis CuONPs formation, at different concentration of copper sulphate. The optimum concentration of $CuSO_4$ was 40 mM

low concentration (10 mM) of copper sulphate there will be low the number of Cu^{2+} ions which have to be reduced to Cu nuclei [31].

FTIR analysis: The FTIR spectra of copper oxide nanoparticles is shown in Fig. 5. The two peaks values at 3537.45, 3471.87, corresponds to N-H stretch amines, suggested that the role of amines in the stabilization of CuO NPs. The absorption peaks at 3406.29, 3055.24, 3016.65, 2881.65, 1728.22, 1639.49, 1539.20, 1285.30 were corresponding to O-H stretch carboxylic group, C-H aromatic, C-H aliphatic, C=O amide groups, C=C, C-N, respectively. These different bands indicate that the presence of alkanes, phenols, carboxylic acid groups, nitro compounds and alcohols, which are responsible for reduction of copper ion to copper nanoparticles by capping materials of plant extract [32]. The three infrared absorption peaks reveal the vibrational modes of CuO nanostructures in the range of 700-400 cm^{-1}. The major peaks were observed to be 489.92, 536.21 and 586.36 cm^{-1}. The present FTIR spectrum is well consistent with that of CuO reported in the previous work of literatures [33].

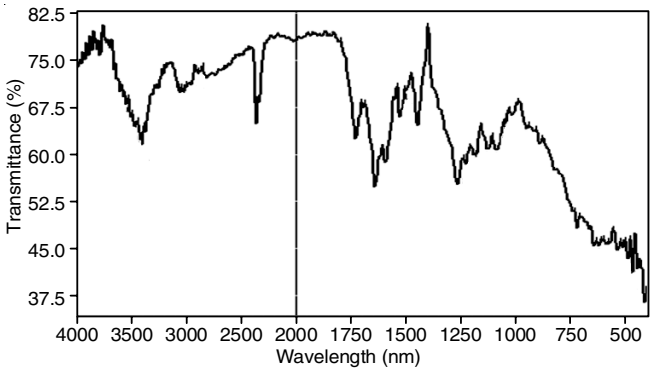

Fig. 5. FTIR spectra of CuONPs

X-ray diffraction analysis: The XRD analysis of synthesized CuO nanoparticles from *Cordia myxa* L. leaf extract is shown (Fig. 6) a series of diffraction peaks at 2θ of 32.49, 38.55, 44.27, 52.81, 59.35, 62.17, 68.68 and 74.35 which were assigned to planes 110, 111, 202, 020, 202, 113, 220 and 004 planes, respectively. The sharp and narrow diffraction peaks indicating highly crystalline structure nature of nanoparticles,

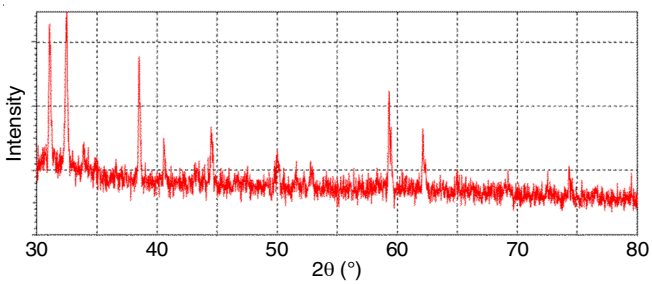

Fig. 6. X-ray pattern of CuONPs

which are in good agreement with those of powder CuO obtained from the international center of diffraction data card (JCPDS). The average crystallite size is found to be 27.2 nm with size ranging from 15 to 48 nm. The X-ray study indicate that the resultant copper oxide nanoparticles are crystalline and identical to monoclinic structure [34].

Scanning electron microscope (SEM) analysis: The scanning electron microscope showed particles were spherical in shape, ranged 20-35 nm (Fig. 7). Our result is in agreement with other literature [35]. Large nanoparticles were seen due to aggregation. This aggregation took place due to the presence of cell components on the surface of nanoparticles and acts as capping agent [36]. The EDX analysis of copper oxide nanoparticles synthesized from the extract of *Cordia myxa* is shown in Fig. 8. The EDAX spectrum was recorded in the spot-profile mode, which indicated the reduction of copper ions to a copper oxide in the reaction mixture. The optical absorption peak is observed at 1 Kev, which is typical for the absorption of metallic copper nanoparticles [37]. Strong signals from the copper and oxygen atoms are observed, while weaker signals for elements Al and Si along with copper and oxygen. The weak signals of silica and aluminum in figures of EDX are due to the aluminum grid base used for analysis and silica holder used during spectral sample preparation and these are considered preparation transport impurities [38]. The atomic and the weight percentage of Cu and O are 5.49, 93.63, 1.45 and 98.02, respectively.

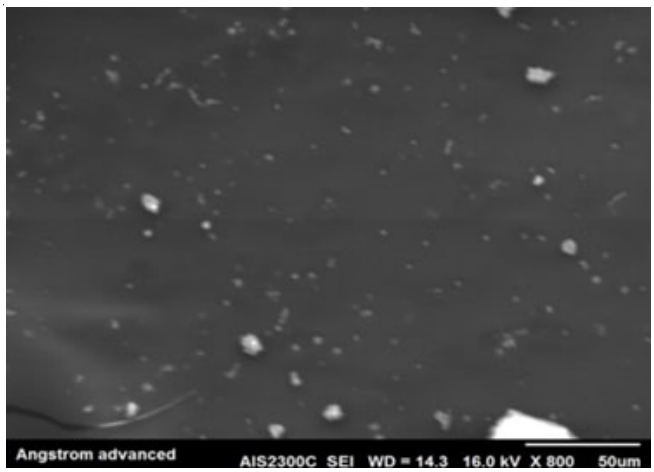

Fig. 7. SEM image of CuONPs

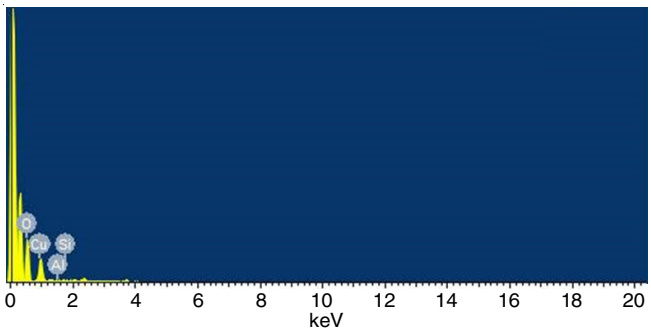

Fig. 8. EDX spectra of CuONPs

Atomic force microscopy analysis: Atomic force microscopy was used to monitor the samples morphology and roughness of the copper oxide nanoparticles (Fig. 9). The micrographs clearly indicate that the formulated copper oxide possess spherical shape and have the calculated grain size in the range between (20-106) nm in diameter with the mean size 85.8 nm. Wider scans covering a few micrometers yielded a root mean square (RMS) roughness of 23.5 nm with a maximum value 106 nm. This grain size was much bigger than that

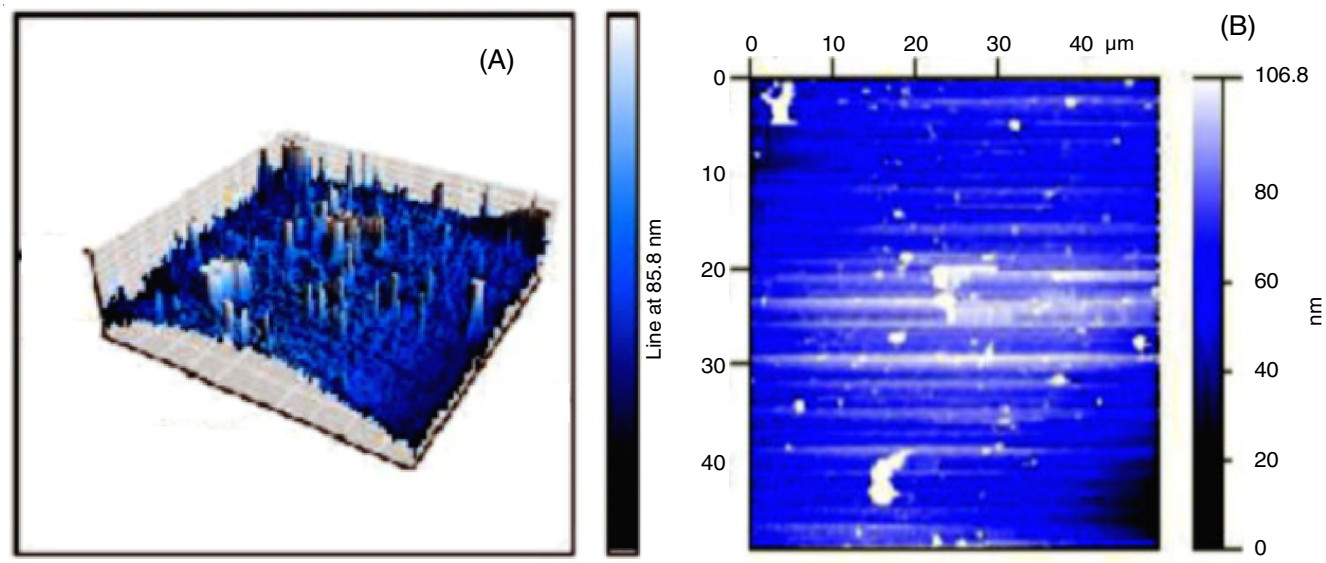

Fig. 9. AFM image of CuONPs, (A) 3D topographical map of CuONPs showing irregularities surface (B) showing well dispersed and size of NPs

of evaluated values from SEM images. This enlargement in the grain size may be due to the involution of true particle size with that of the AFM point and also on the preparation of samples for AFM [39].

Conclusion

A simple and low cost approach for the preparation of copper oxide nanoparticles was employed successfully using aqueous extract of *Cordia myxa* L. leaves as reducing, stabilizing and capping agent. The biosynthesized nanoparticles have been characterized by UV-visible, XRD, FTIR, SEM, EDS and AFM. The reaction conditions including volume ratio of plant extract and salt, pH and concentration of copper sulphate were optimized in order to get the CuO NPs.

ACKNOWLEDGEMENTS

The authors thank Dr. Amer T. Tawfeeq, for proof reading of the manuscript.

REFERENCES

1. K. Zhou, R. Wang, B. Xu and Y. Li, *Nanotechnology*, **17**, 3939 (2006); https://doi.org/10.1088/0957-4484/17/15/055.
2. A. Hedayati, H. Kolangi, A. Jahanbakhshi and F. Shaluei, *Bulg. J. Vet. Med.*, **15**, 172 (2012).
3. K. Inouea, H. Takano, R. Yanagisawa, E. Koike and A. Shimada *Toxicol. Appl. Pharmacol.*, **234**, 68 (2009); https://doi.org/10.1016/j.taap.2008.09.012.
4. K.S. Khashan, G.M. Sulaiman and F.A. Abdulameer, *Arab. J. Sci. Eng.*, **41**, 301 (2016); https://doi.org/10.1007/s13369-015-1733-7.
5. J. Park, J.S.G. Joo, S.G. Kwon, Y. Jang and T. Hyeon, *Chem. Int. Ed*, **46**, 4630 (2007); https://doi.org/10.1002/anie.200603148.
6. F. Marabelli, G.B. Parravicini and F. Salghetti-Drioli, *Phys. Rev. B*, **52**, 1433 (1995); https://doi.org/10.1103/PhysRevB.52.1433.
7. H. El-Trass, I. Elshamy, I. El-Mehasseb and M. El-Kemary, *Appl. Surf. Sci.*, **258**, 2997 (2012); https://doi.org/10.1016/j.apsusc.2011.11.025.
8. M.J. Guajardo-Pacheco, J.E. Morales-Sánchez, J. González-Hernández and F. Ruiz, *Mater. Lett.*, **64**, 1361 (2010); https://doi.org/10.1016/j.matlet.2010.03.029.
9. N. Kröger, R. Deutzmann and M. Sumper, *Science*, **286**, 1129 (1999); https://doi.org/10.1126/science.286.5442.1129.
10. G.A.K. Reddy, J.M. Joy, T. Mitra, S. Shabnam and T. Shilpa, *Int. J. Adv. Pharm.*, **2**, 9 (2012).
11. S. Iravani, *Green Chem.*, **13**, 2638 (2011); https://doi.org/10.1039/c1gc15386b.
12. J. Huang, Q. Li, D. Sun, Y. Lu, Y. Su, X. Yang, H. Wang, Y. Wang, W. Shao and N. He, *Nanotechnology*, **18**, 105104 (2007); https://doi.org/10.1088/0957-4484/18/10/105104.
13. M. Ranjbar, H.N. Varzi, A. Sabbagh, A. Bolooki and A. Sazmand, *Pak. J. Biol. Sci.*, **16**, 2066 (2013); https://doi.org/10.3923/pjbs.2013.2066.2069.
14. B. Anuj, A. Rajalakshmi, N. Krithega, S. Gurupavaithra and A. Jayachitra, *Int. J. Biol. Pharm. Res.*, **5**, 511 (2014).
15. U. Holzwarth and N. Gibson, *Nat. Nanotechnol.*, **6**, 534 (2011); https://doi.org/10.1038/nnano.2011.145.
16. S. Shankar, A. Rai, B. Ankamwar, A. Singh, A. Ahmad and M. Sastry, *Nat. Mater.*, **3**, 482 (2004); https://doi.org/10.1038/nmat1152.
17. M.A. Noginov, G. Zhu, M. Bahoura, J. Adegoke, C. Small, B.A. Ritzo, V.P. Drachev and V.M. Shalaev, *Appl. Phys. B*, **86**, 455 (2007); https://doi.org/10.1007/s00340-006-2401-0.
18. H.R. Naika, K. Lingaraju, K. Manjunath, D. Kumar, G. Nagaraju, D. Suresh and H. Nagabhushana, *J. Taibah Univ. Sci.*, **9**, 7 (2015); https://doi.org/10.1016/j.jtusci.2014.04.006.
19. R. Cuevas, N. Duran, M.C. Diez, G.R. Tortella and O. Rubilar, *J. Nanomater.*, **2015**, 1 (2015); https://doi.org/10.1155/2015/789089.
20. A. Moores and F. Goettmann, *New J. Chem.*, **30**, 1121 (2006); https://doi.org/10.1039/b604038c.
21. G. Mie, *Ann. Phys.*, **330**, 377 (1908); https://doi.org/10.1002/andp.19083300302.
22. N.T.K. Thanh, N. Maclean and S. Mahiddine, *Chem. Rev.*, **114**, 7610 (2014); https://doi.org/10.1021/cr400544s.
23. D. Mott, J. Luo, A. Smith, P.N. Njoki, L. Wang and C.J. Zhong, *Nanoscale Res. Lett.*, **2**, 12 (2007); https://doi.org/10.1007/s11671-006-9022-8.
24. D. Mott, J. Galkowski, L. Wang, J. Luo and C.J. Zhong, *Langmuir*, **23**, 5740 (2007); https://doi.org/10.1021/la0635092.
25. G. Caroling, M.N. Priyadharshini, E. Vinodhini, A.M. Ranjitham and P. Shanthi, *Int. J. Pharm. Biol. Sci.*, **5**, 25 (2015).
26. T.K. Sau, A. Pal and T. Pal, *J. Phys. Chem. B*, **105**, 9266 (2001); https://doi.org/10.1021/jp011420t.
27. R.A. Soomro, S.T. Hussain, S. Sirajuddin, N. Memon, M.R. Shah, N.H. Kalwar, K.R. Hallam and A. Sha, *Adv. Mat. Lett.*, **5**, 191 (2014); https://doi.org/10.5185/amlett.2013.8541.
28. N.I. Hulkoti and T.C. Taranath, *Colloids Surf. B Biointerfaces*, **121**, 474 (2014); https://doi.org/10.1016/j.colsurfb.2014.05.027.
29. M. Sathishkumar, K. Sneha and Y.S. Yun, *Bioresour. Technol.*, **101**, 7958 (2010); https://doi.org/10.1016/j.biortech.2010.05.051.
30. S.P. Dubey, M. Lahtinen and M. Sillanpaa, *Process Biochem.*, **45**, 1065 (2010); https://doi.org/10.1016/j.procbio.2010.03.024.
31. M.R. Salvadori, L.F. Lepre, R.A. Ando, C.A.O. do Nascimento and B. Correa, *PLoS One*, **8**, e80519 (2013) https://doi.org/10.1371/journal.pone.0080519.
32. K.B. Narayanan and N. Sakthivel, *Mater. Charact.*, **61**, 1232 (2010); https://doi.org/10.1016/j.matchar.2010.08.003.
33. K. Karthik, N.V. Jaya, M. Kanagaraj and S. Arumugam, *Solid State Commun.*, **151**, 564 (2011); https://doi.org/10.1016/j.ssc.2011.01.008.
34. A. Ahmed, P. Elvatia and A. Violi, *RSC Adv.*, **5**, 35033 (2015); https://doi.org/10.1039/C5RA04276C.
35. R. Dastjerdi and M. Montazer, *Colloids Surf. B Biointerfaces*, **79**, 5 (2010); https://doi.org/10.1016/j.colsurfb.2010.03.029.
36. D. Sharma, S. Kanchi and K. Bisetty, *Arab. J. Chem.*, (2015); https://doi.org/10.1016/j.arabjc.2015.11.002.
37. T. Raju and P. Sabhapathy, *Asian J. Chem.*, **27**, 23 (2015); https://doi.org/10.14233/ajchem.2015.16657.
38. K.L. Niraimath, R. Lavany, V. Sudh, R. Narendra and P. Brindh, *J. Pharm. Res.*, **10**, 29 (2016).
39. P. Eaton, P. Quaresma, C. Soares, C. Neves, M.P. de Almeida, E. Pereira and P. West, *Ultramicroscopy*, **182**, 179 (2017); https://doi.org/10.1016/j.ultramic.2017.07.001.